

Condensation of Free Excitons into Electron-Hole Drops in Pure Germanium[†]

C. Benoît à la Guillaume and M. Voos

Groupe de Physique des Solides de l'Ecole Normale Supérieure,
Tour 23, 5 Place Jussieu, Paris 5e, France*

and

F. Salvan

Centre Universitaire de Luminy, Marseille, France

(Received 28 October 1971)

A simple theory is given to justify the existence, in intrinsic semiconductors, of electron-hole drops (EHD) resulting from the condensation of free excitons. It is shown that such a condensation is favored by a multivalley band structure. The critical density n_c of electron-hole pairs in EHD is then determined in pure Ge from luminescence experiments and it is compared to other data. This study shows that n_c is of the order of $2 \times 10^{17} \text{ cm}^{-3}$ in this material. We also investigate the light emission of EHD in uniaxially stressed Ge. The results obtained are interpreted from the stress variation of n_c and they are shown to be consistent with the EHD theoretical model. In addition, we study, in the same material, the temperature dependence of the EHD total lifetime. Finally, we briefly discuss the case of Si with respect to the EHD model.

I. INTRODUCTION

In usual intrinsic semiconductors the lowest-energy electronic excitation is the free exciton (hereafter called FE) which is described in the Wannier approximation. If several excitons are present in the crystal, their mutual interaction seems to be attractive and this may lead to bound states. The first one which has been proposed is the excitonic molecule,^{1,2} which is a complex resulting from the binding of two FE. The second one, which has been introduced by Keldysh,³ is a kind of electron-hole "liquid" and corresponds to the condensation of FE into electron-hole drops (hereafter called EHD).

We wish to report here some elementary theoretical considerations to justify the occurrence of such a liquid phase. We show on a simple model that a multivalley band structure is a favorable situation for the stability of EHD whose existence has been clearly demonstrated in Ge from photo-voltaic-detection^{4,5} and light-scattering⁶ experiments. We also examine theoretically the radiative-recombination properties of EHD in the case of the indirect semiconductor Ge.

Since the critical density n_c of electron-hole pairs in EHD is an important parameter, we discuss rapidly the experimental values of n_c obtained by several authors⁷⁻⁹ in Ge and we report new determinations of this density. It is noteworthy that our results are derived from the optical properties of EHD as are most of the measurements of n_c which have been already performed. We also investigate the light emission of EHD in uniaxially stressed samples of Ge to study the variation of n_c with stress. Our results are interpreted from

the band-structure modifications which occur when uniaxial stresses are applied and they are shown to be qualitatively in good agreement with the EHD theoretical model. In addition we study the temperature dependence of the total lifetime of EHD in the same material, and the data obtained are interpreted by taking into account the evaporation of FE at the drop surface. Finally, we examine and we discuss rapidly the experimental situation in Si with respect to the EHD model.

II. THEORETICAL CONSIDERATIONS

A. Stability of EHD

The simplest case which can be considered is that of a neutral plasma in which the density n of electron-hole pairs is large and corresponds to $na_0^3 > 1$, where a_0 is the Bohr radius of a FE. When this condition is satisfied, the FE cannot exist and the system may be considered as a two-component plasma which can be described in the Hartree-Fock approximation (at $T=0$). In this approximation, the mean energy per pair $\langle E_n \rangle$ can be calculated as a function of the density n in the supposedly homogeneous medium. It is noteworthy that in this case the direct electron-electron and hole-hole Coulomb terms cancel with the electron-hole term. Therefore, $\langle E_n \rangle$ can be written

$$\langle E_n \rangle = E_g + \langle E_{\mathbf{k}1n}^e \rangle + \langle E_{\mathbf{k}1n}^h \rangle - \langle E_{\mathbf{ex}}^e \rangle - \langle E_{\mathbf{ex}}^h \rangle + \langle E_{\text{cor}} \rangle, \quad (1)$$

where E_g is the band gap, $\langle E_{\mathbf{k}1n}^e \rangle$ and $\langle E_{\mathbf{k}1n}^h \rangle$ the mean kinetic energies of electrons and holes, $\langle E_{\mathbf{ex}}^e \rangle$ and $\langle E_{\mathbf{ex}}^h \rangle$ the mean exchange energies of electrons and holes, and $\langle E_{\text{cor}} \rangle$ the mean correlation energy.

If we consider a simple band with a spherical effective mass m^* , we easily find

$$\langle E_{\text{kin}} \rangle = \frac{3}{5} (\hbar^2 k_F^2 / 2m^*) = Bn^{2/3} / m^* \quad (2)$$

and

$$\langle E_{\text{ex}} \rangle = \frac{4\pi e^2}{\epsilon n} \sum_{j,1} \frac{1}{|\mathbf{k}_j - \mathbf{k}_1|^2} = \frac{An^{1/3}}{\epsilon}, \quad (3)$$

where ϵ is the dielectric constant of the medium.

For a simple band structure with spherical bands corresponding to electron and hole effective masses m_e and m_h , one gets from expressions (1)–(3)

$$\langle E_n \rangle = E_g + Bn^{2/3} / \mu - 2An^{1/3} / \epsilon + \langle E_{\text{cor}} \rangle, \quad (4)$$

where

$$1/\mu = 1/m_e + 1/m_h.$$

If r_s is the usual interelectron spacing measured in units of Bohr radii, one can recognize the development of $1/r_s^\alpha$, which is familiar in one-component plasmas. Neglecting $\langle E_{\text{cor}} \rangle$ we can calculate from Eq. (4) the critical density n_c which corresponds to the minimum value $\langle E_n \rangle_m$ of $\langle E_n \rangle$. If the corresponding r_s value is not small, we nevertheless use this method because $\langle E_{\text{cor}} \rangle$ is a slowly varying function of r_s , and we may neglect its variation, even if its absolute value is not very small compared to $\langle E_{\text{kin}} \rangle$ or $\langle E_{\text{ex}} \rangle$. In the simple case considered above, we thus find

$$n_c^{1/3} = (A/B) (\mu/\epsilon) \sim 2 |\phi_{\text{FE}}(\tilde{\mathbf{r}}=0)|^{2/3} \quad (5)$$

and

$$\begin{aligned} \langle E_n \rangle_m &= E_g - (A^2/B) (\mu/\epsilon^2) + \langle E_{\text{cor}} \rangle \\ &\sim E_g - \frac{2}{3} R^* + \langle E_{\text{cor}} \rangle. \end{aligned} \quad (6)$$

In these expressions, R^* is the effective Rydberg of the FE and $|\phi_{\text{FE}}(0)|^2 = 1/64\pi a_0^3$, where $\phi_{\text{FE}}(\tilde{\mathbf{r}})$ is the wave function of the relative electron-hole motion of the FE.

To obtain a condensed phase stable at $T=0$, we need to have $\langle E_n \rangle_m < E_g - R^*$ so that $\langle E_{\text{cor}} \rangle$ must be negative. Now we try a more complicated band structure to see if, neglecting $\langle E_{\text{cor}} \rangle$, a more favorable situation can be obtained. Therefore, we consider one spherical hole band with mass m_h and four spherical electron bands with mass m_e for each valley. In that case, we find

$$\begin{aligned} \langle E_n \rangle &= E_g + Bn^{2/3} \left(\frac{1}{m_h} + \frac{1}{4^{2/3} m_e} \right) \\ &\quad - \frac{An^{1/3}}{\epsilon} \left(1 + \frac{1}{4^{1/3}} \right) + \langle E_{\text{cor}} \rangle. \end{aligned} \quad (7)$$

If $\sigma = m_h/m_e$, one gets

$$\frac{n_{c,4}^{1/3}}{n_{c,1}^{1/3}} = 0.82 \frac{1+\sigma}{1+0.4\sigma} \quad (8)$$

and

$$\frac{\langle E_n \rangle_{m,4} - E_g}{\langle E_n \rangle_{m,1} - E_g} = 0.67 \frac{1+\sigma}{1+0.4\sigma}, \quad (9)$$

where the subscripts 1 and 4 refer, respectively, to 1 and 4 valleys.

The multivalley structure is therefore favorable if σ is large enough, and this could be the case for Ge. One has also to take into account the anisotropy of the conduction band and the degeneracy of the valence band. It has been shown by Nozières and Combescot¹⁰ that the exchange term can be calculated exactly in this material. In the conduction band, the effect of the anisotropy ($m_{\parallel}/m_{\perp} \approx 20$) is to reduce the electron exchange term by a factor 0.84. In the valence band the degeneracy causes a reduction of the hole exchange term by a factor 0.77. They have also performed more complicated calculations¹⁰ which take into account the correlation energy. Their results, which are in good agreement with experiment, show that the correlation term is also favored by a multivalley band structure.

If the correlation energy is neglected, $\langle E_n \rangle_m - E_g$ is near 2 meV. Since $R^* = 3.6$ meV¹¹ in Ge, $\langle E_{\text{cor}} \rangle$ must be negative if we want to reach the situation which is sketched in Fig. 1. At low n the more stable state is the FE gas but, when n is increased, the attractive interaction causes a decrease of $\langle E_n \rangle$ and, at $n = n_c$, an absolute minimum of $\langle E_n \rangle$ would be obtained. For $n > n_c$, the Hartree-Fock approximation is more and more valid, and $\langle E_n \rangle$ increases because the kinetic energy term becomes the dominant one. Then, if one considers a given volume occupied by a mean density lying between 0 and n_c at $T=0$, the system will separate into two phases: an FE gas of low density ($n \approx 0$) and a phase at the density n_c . Such a phase, where the

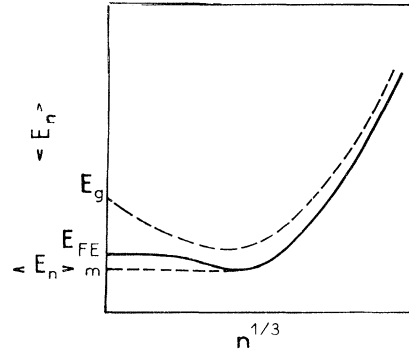


FIG. 1. Solid line represents the general behavior at $T=0$ of the mean energy per pair $\langle E_n \rangle$ vs $n^{1/3}$ when $\langle E_{\text{cor}} \rangle$ is taken into account. E_{FE} is the FE energy. The minimum of that curve occurs for $n=n_c$. The dashed line gives $\langle E_n \rangle$ when $\langle E_{\text{cor}} \rangle$ is neglected.

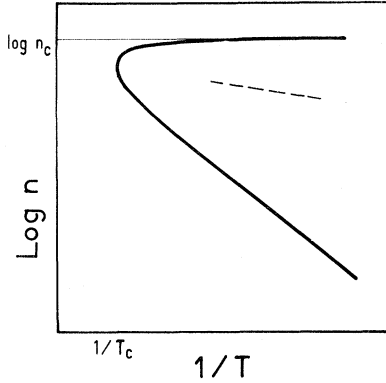


FIG. 2. Usual liquid-gas phase diagram. T_c is the critical temperature and the dashed line would correspond to the Mott transition in an homogeneous system.

density is imposed and where both kinds of particles have nearly equal masses, should be analogous to a liquid metal. Of course, at a finite temperature, the entropy term has to be considered in analogy with ordinary liquid-gas transformations and the usual liquid-gas phase diagram represented in Fig. 2 should result.

There is some analogy with the Mott transition since as n increases one goes from a nonconducting phase, where each electron is bound to a particular hole, to a conducting phase, where a given electron is no more bound to any particular hole. But there is in fact one difference with the Mott transition. Indeed in the case of EHD, the two kinds of particles can move easily. This is why the system can separate into two phases if $n_s < n < n_c$, where n_s is the density of the FE gas at saturation at the temperature considered.

B. Radiative-Recombination Properties of EHD

In this section we examine the radiative-recombination properties of EHD in an indirect band-gap semiconductor such as Ge. We can calculate the EHD spectrum $I(h\nu)$ and the corresponding total intensity I in the case of a radiative-recombination mechanism involving the emission of one particular phonon $\hbar\omega$. If \vec{k}_e and \vec{k}_h are the momenta with respect to the band extrema of electrons and holes involved in such a process and if we consider only one intermediate state, $I(h\nu)$ and I are thus given at $T = 0$ by

$$I(h\nu) = (|D|^2 / |\Delta E|^2) \int_{V_h} \int_{V_e} |H(\vec{k}_e, \vec{k}_h)|^2 \times \delta(h\nu - E_g - E_{\vec{k}_{in}}^e - E_{\vec{k}_{in}}^h + \hbar\omega) d\vec{k}_e d\vec{k}_h \quad (10)$$

and

$$I = (|D|^2 / |\Delta E|^2) \int_{V_h} \int_{V_e} |H(\vec{k}_e, \vec{k}_h)|^2 d\vec{k}_e d\vec{k}_h, \quad (11)$$

where D is the optical matrix element, ΔE the usual

energy denominator, V_h and V_e the volumes inside the hole and electron Fermi surfaces, and $H(\vec{k}_e, \vec{k}_h)$ the electron-phonon matrix element.

In the case of an allowed phonon process (LA or TO phonon in Ge), $|H(\vec{k}_e, \vec{k}_h)|^2$ is constant¹² and we take it equal to $|H|^2$. Equation (10) can be used⁷ to find n_c from the experimental spectrum if one neglects the k dependence of the exchange and correlation energies. In fact it is known that in a one-component plasma $\langle E_{ex} \rangle + \langle E_{cor} \rangle$ is nearly k independent,¹³ but we do not know if this property is preserved in a two component plasma.

Since the main radiative processes correspond to allowed phonons, the squared matrix element $|\gamma|^2$ for the radiative recombination of a given electron in an EHD does not depend on \vec{k}_e . It can be written

$$|\gamma|^2 = \frac{|D|^2}{|\Delta E|^2} |H|^2 \int_{V_h} d\vec{k}_h = \frac{|D|^2}{|\Delta E|^2} |H|^2 n_c. \quad (12)$$

Let us consider now the case of an FE whose wave function is given by

$$\sum_{\vec{k}} a_{\vec{k}} \phi_{v,\vec{k}}(\vec{r}_h) \phi_{c,\vec{k}+\vec{K}}(\vec{r}_e), \quad (13)$$

where v and c refer, respectively, to the valence and conduction bands, and \vec{r}_h and \vec{r}_e to the hole and the electron of the FE.

The squared matrix element $|\gamma'|^2$ for the radiative recombination of an FE is thus found to be

$$|\gamma'|^2 = \frac{|D|^2}{|\Delta E|^2} |H|^2 \left| \sum_{\vec{k}} a_{\vec{k}} \right|^2 = \frac{|D|^2}{|\Delta E|^2} |H|^2 |\phi_{FE}(0)|^2. \quad (14)$$

This allows us to determine the ratio of the FE and EHD radiative lifetimes which are called τ_R^{FE} and τ_R^{EHD} , respectively:

$$\tau_R^{FE} / \tau_R^{EHD} = |\gamma|^2 / |\gamma'|^2 = n_c / |\phi_{FE}(0)|^2. \quad (15)$$

It must be noted that this relation provides an other method to measure n_c .

In Ge, in addition to the main recombination mechanism which involves an LA phonon, there is also a TA-phonon-assisted process which is, in fact, forbidden for an electron-hole pair at the band extrema.¹² In this case, the corresponding electron-phonon matrix element can be developed as follows for small \vec{k}_e and \vec{k}_h :

$$H_{TA}(\vec{k}_e, \vec{k}_h) = \vec{M}_e \cdot \vec{k}_e + \vec{M}_h \cdot \vec{k}_h + \dots \quad (16)$$

Obviously the over-all intensity of the TA-assisted recombination radiation of an object constituted by electron-hole pairs will depend on the extension of that object in k space. It is possible to compare the intensities I_{TA} and I_{LA} corresponding, respectively, to the TA- and LA-assisted processes in the case of a thermal population of FE at temperature T and also in the case of EHD. For an FE of total momentum \vec{K} , the following relation is

easily found:

$$|H_{TA}|^2 / |H_{LA}|^2 \approx |(\vec{M}_e - \vec{M}_h) \cdot (\vec{K} - \vec{K}_M)|^2 / |H_{LA}|^2, \quad (17)$$

where H_{LA} is the electron-phonon matrix element of the LA-assisted process and \vec{K}_M is the momentum of the FE at the band extrema.

The average value of this ratio over a thermal repartition of FE at temperature T yields the following relation:

$$\left(\frac{I_{TA}}{I_{LA}} \right)_{FE} \approx \frac{|\vec{M}_e - \vec{M}_h|^2}{|H_{LA}|^2} \frac{mkT}{\hbar^2} \quad (18)$$

when m , which is the total mass of FE, is assumed to be isotropic.

In the case of EHD, considering the large anisotropy of the electron effective mass, we assume that the most important term in H_{TA} will be $M_{e_z} k_{e_z}$, where z is along $\langle 111 \rangle$. We thus find

$$\left(\frac{I_{TA}}{I_{LA}} \right)_{EHD} \approx \frac{M_{e_z}^2}{|H_{LA}|^2} \frac{\int_{V_e} k_{e_z}^2 d\vec{k}_e}{\int_{V_e} d\vec{k}_e}. \quad (19)$$

Equation (19) yields finally

$$(I_{TA}/I_{LA})_{EHD} \approx (5.5 M_{e_z}^2 / |H_{LA}|^2) n_c^{2/3}. \quad (20)$$

III. EXPERIMENTAL TECHNIQUES

In our experiments, the excitation source was either a 100-W high-pressure mercury lamp or a pulsed GaAs laser whose peak power was approximately 10 W. The laser pulse length was 1 μ sec with a fall time smaller than 0.1 μ sec and the pulse repetition rate was 200 Hz. The Ge samples, which were etched with CP4 and rinsed in distilled water, were immersed in pumped liquid or gaseous helium. The light emission from the irradiated surface was detected and it was analyzed, in some experiments performed with the mercury lamp or the GaAs laser, with a spectrometer equipped with a cooled lead sulphide photodetector. In other experiments using the GaAs laser to measure luminescence decay times, the recombination light emerging from the sample fell on a fast detector, this was a Ge photodiode with a fall time of 0.2 μ sec. This photodiode was followed by a box-car integrator to analyze the detected signals as a function of time. Let us add that all our experimental results were obtained in pure Ge with residual impurity concentrations smaller than 10^{13} cm^{-3} .

IV. EXPERIMENTAL RESULTS AND DISCUSSION

In fact, the first experimental evidence of new bound states in intrinsic semiconductors was the occurrence of new radiative-recombination lines at low temperature in Si² and Ge^{14,15} as shown in Fig. 3 in the case of Ge. The excitonic-molecule model was proposed to interpret these lines,^{2,15} essen-

tially on the basis of qualitative arguments. However, it is now clear that EHD do exist⁴⁻⁶ in pure Ge at low temperature. In addition, the light scattering experiment of Pokrovskii and Svistunova⁶ shows that it is easy to get a situation where most of the created holes are actually in the EHD phase. Only the new recombination lines are observed in these conditions, and they are, therefore, due to EHD since the calculations of Sec. II B show that the EHD can radiate. Besides, radiative-recombination spectra taken in a wide range of temperature and excitation have not exhibited other lines than the FE and EHD ones. Since the emission spectrum of excitonic molecules should be different, we do not have any proof¹⁶ of the possible existence of this complex in Ge.

A. Determination of n_c in EHD

We give here experimental determinations of the critical density n_c in pure Ge. These values were determined from the TA- and LA-phonon-assisted-emission lines of EHD and also from the study of the FE and EHD radiative lifetimes. Also, we compare our data to the results obtained by several authors⁷⁻⁹ who have used other measurement methods.

(i) *Intensity ratio of the TA- and LA-assisted lines.* Figure 4 represents the TA- and LA-phonon-assisted lines of EHD at 2°K. The ratio of the integrated intensities of these two lines is 0.065, while the ratio for FE is 0.055¹⁷ at 20°K. It is possible to use these results to get n_c from Eqs. (18) and (20). If we assume that $|\vec{M}_e - \vec{M}_h|^2$ is of the order of $M_{e_z}^2$ we find $n_c \approx 1.8 \times 10^{17} \text{ cm}^{-3}$.

(ii) *Radiative lifetime.* We have measured^{18,19}

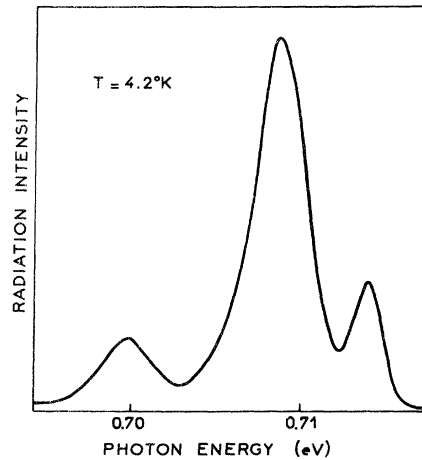


FIG. 3. Radiative-recombination spectrum of pure Ge at 4.2°K. The emission peak at 713.6 meV corresponds to the FE and the two other peaks are the new emission lines.

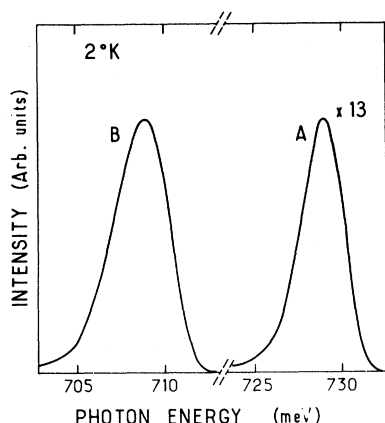


FIG. 4. Luminescence spectrum of EHD in pure Ge at 2°K. Curve A corresponds to the TA-phonon-assisted emission line and curve B to the LA-phonon-assisted one.

the ratio of the FE and EHD radiative lifetimes which has been found to be equal to about 16. From that result and from Eq. (15) we readily obtain $n_c \approx 1.6 \times 10^{17} \text{ cm}^{-3}$ since $|\phi_{FE}(0)|^2 \sim 10^{16} \text{ cm}^{-3}$ in Ge.

(iii) *Radiative recombination spectrum.* Pokrovsky *et al.*⁷ have calculated the shape of the LA-phonon-assisted line of EHD. They have found a good fit between experiment and theory for $n_c = 2.6 \times 10^{17} \text{ cm}^{-3}$.

(iv) *Plasma frequency in EHD.* From the determination of the plasma frequency in EHD, Vavilov *et al.*⁸ have deduced that n_c is of the order of $2 \times 10^{17} \text{ cm}^{-3}$.

(v) *Electrical conductivity.* Rogachev⁹ has observed an abrupt jump of the conductivity at low temperature when n becomes larger than $2 \times 10^{16} \text{ cm}^{-3}$. If one considers that the system is composed of an insulating FE gas and some highly conducting EHD, the calculation of the corresponding conductivity is thus a typical percolation problem. It is known that in this case the conductivity jump must occur when the volume occupied by the EHD is larger than 0.15 times the total volume.²⁰ This gives $0.15 n_c \approx 2 \times 10^{16} \text{ cm}^{-3}$ so that $n_c \approx 1.35 \times 10^{17} \text{ cm}^{-3}$.

All these determinations of n_c are, therefore, in good agreement. The precision on n_c is limited either by the experimental accuracy as in the case of the determination of the ratio of the FE and EHD radiative lifetimes, or by the lack of a more sophisticated theory which would allow us to deduce a better value of n_c from experimental results as in the case of the comparison of the LA- and TA-phonon-assisted processes. At the moment, a value of $(1.95 \pm 0.65) \times 10^{17} \text{ cm}^{-3}$ seems to fix the limit of the n_c value in Ge.

B. Variation of n_c with a Uniaxial Stress

Since the previous simple theory (given in Sec. II A) has shown the effect of a multivalley structure on n_c and $\langle E_n \rangle_m - E_g$, it is interesting to modify this structure by applying uniaxial compressive stresses which lift the degeneracies of the conduction and valence bands in Ge.

At first we have measured, as a function of the applied stress, the variation of the initial signal emitted at 2°K by the EHD just at the end of the exciting pulse. In these experiments, the formation time of EHD is shorter than $1 \mu\text{sec}$.¹⁹ In addition, since the total lifetime¹⁹ is much larger than the excitation pulse length, the amount of recombination at the end of that pulse is negligible. It is thus clear that the initial signal is emitted by a constant number of pairs condensed in EHD. This signal is proportional to their radiative-recombination probability, and consequently to n_c as shown in Sec. II B. Figure 5, which represents the stress dependence of this initial signal, describes therefore the variation of n_c with the applied uniaxial pressure P . From the elementary theory given in Sec. II A we can justify the change of n_c with a $\langle 100 \rangle$ stress just on the basis of the valence-band splitting which is equivalent to a lowering of the hole mass²¹ and to a decrease of σ in Eqs. (8) and (9). For stresses in the $\langle 111 \rangle$ direction, we have, in addition, an energy lowering of one conduction-band valley which produces a larger decrease of n_c since we go from the four-valley case to the one-valley case.

We have also studied at 2°K the stress-induced modifications of the EHD radiative-recombination spectrum. Figure 6 gives the shift of the maximum of the EHD main emission line versus the ap-

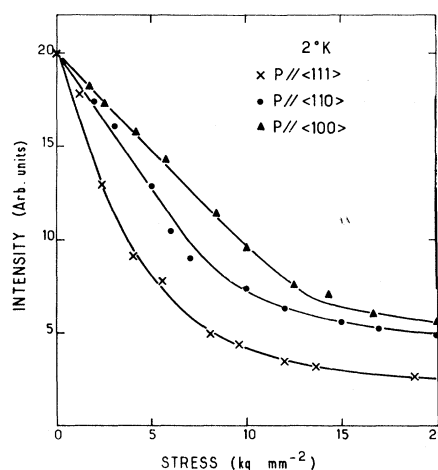


FIG. 5. Intensity of the initial signal emitted by EHD as a function of the applied uniaxial pressure.

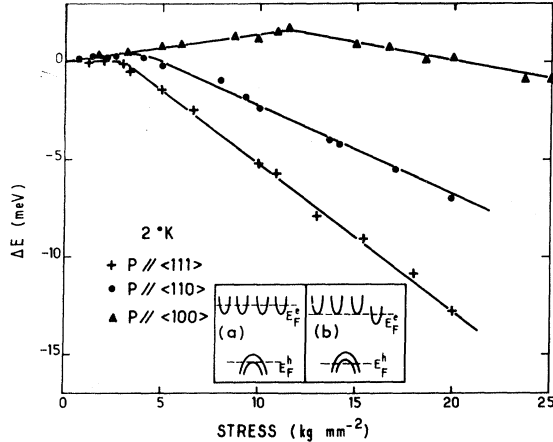


FIG. 6. Energy displacement ΔE of the EHD main emission peak as a function of the applied uniaxial stress. Schemes (a) and (b) correspond, respectively, to the situations occurring for $P=11.5 \text{ kg mm}^{-2}$ in the $\langle 100 \rangle$ direction and for $P=3 \text{ kg mm}^{-2}$ in the $\langle 111 \rangle$ direction.

plied pressure, and Fig. 7 represents the variations with stress of the half-width of this line. The results presented in Fig. 6 show that for relatively high pressures the shift of the EHD radiation peak is approximately similar to that of the FE one²² as could be expected. For lower stresses, the behavior of the EHD line is quite different. In this case, the EHD line does not shift towards low energies because the decrease of the band gap with the applied pressure competes with the reduction of the mean binding energy of electron-hole pairs in the drop. This mean energy decreases since n_c decreases when uniaxial stresses are applied in the $\langle 111 \rangle$, $\langle 110 \rangle$, or $\langle 100 \rangle$ crystallographic directions. It must be pointed out that the shift of the EHD emission peak should become gradually parallel to that of the FE one. Indeed m_h and n_c must decrease as long as the valence-band splitting is not much larger than the hole Fermi energy. However the accuracy of these experiments is not sufficient to detect unambiguously this effect which can nevertheless be observed in Fig. 5.

The change which occurs in the $\langle 100 \rangle$ case near 11.5 kg mm^{-2} in the slope of the curve giving the shift of the EHD radiation peak (Fig. 6) corresponds to the coincidence of the hole Fermi level with the extremum of the lowest-energy valence band resulting from the splitting due to the applied stress. Let us note that our results are slightly different from those reported by Bagaev *et al.*²³ who have observed the same effect for $P \sim 6.5 \text{ kg mm}^{-2}$. The change occurring for $P=3 \text{ kg mm}^{-2}$ in the slope of the curve corresponding to a uniaxial pressure in the $\langle 111 \rangle$ direction corresponds to the coincidence of the electron Fermi level in the lowest-energy

conduction-band valley with the bottom of the three other equivalent valleys. It is easy to get n_c at this pressure since we know that the Fermi energy of electrons which are all in one valley is 3.18 meV .²² We thus find $n_c = 1.1 \times 10^{17} \text{ cm}^{-3}$ for $P=3 \text{ kg mm}^{-2}$. From this value and from Fig. 5, it is then possible to get n_c at $P=0$. We obtain $n_c \approx 1.9 \times 10^{17} \text{ cm}^{-3}$. The same calculations can be performed in the $\langle 100 \rangle$ case by taking into account the stress dependence of the hole effective mass.²⁴ For this pressure direction we get $n_c \approx 4.5 \times 10^{16} \text{ cm}^{-3}$ at $P=11.5 \text{ kg mm}^{-2}$, which yields $n_c \approx 1.1 \times 10^{17} \text{ cm}^{-3}$ but the hole effective mass that we have used is not very correct because the hole Fermi energy is equal to the valence-band splitting. It can nevertheless be noticed that the zero-stress values obtained here for n_c are in rather good agreement with the results of the previous section.

The change of n_c with stress is also observed in Fig. 7. It corresponds to a decrease of the EHD linewidth which should vary as $n_c^{2/3}$. It is likely that the linewidth increase which is observed for large pressures is related to stress inhomogeneities which would be of the order of $10^{-1} P$. Finally, let us add that we have often observed anomalous shifts, broadenings, and even splittings of the EHD emission line which seem to be due to stress inhomogeneities. For this reason, a lot of experiments have been necessary to obtain the typical results reported here which correspond to experimental conditions where these inhomogeneities were not too important.

Figure 8 gives informations about the change with pressure of the EHD total lifetime τ^{EHD} which is given by the luminescence decay time. This lifetime is related to nonradiative processes except at low pressure where the efficiency is near 50%.¹⁹ In fact, it seems difficult to explain such

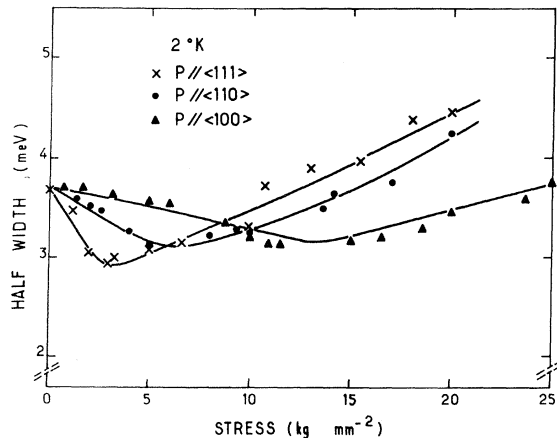


FIG. 7. Variation of the half-width of the EHD main emission peak as a function of the applied uniaxial stress.

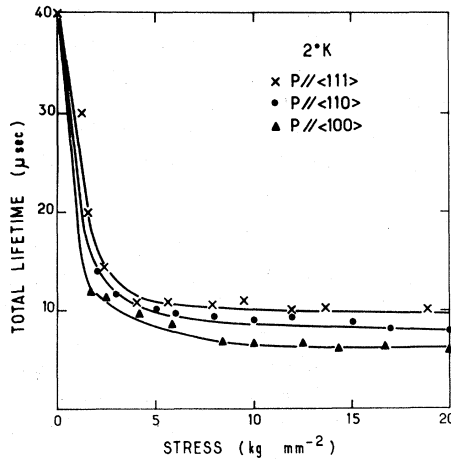


FIG. 8. Total lifetime of EHD vs the applied uniaxial stress.

a rapid variation of τ^{EHD} by a bulk mechanism. It has been observed at $P=0$ that τ^{EHD} is shorter in thin samples, and this fact seems to demonstrate that surface effects may be important. When a stress is applied, it might happen that a stress gradient arises and pushes the EHD toward the surface. Surface-recombination mechanisms could thus rapidly dominate and cause τ^{EHD} to decrease, as shown in Fig. 8. The origin of the $P=0$ non-radiative process is not yet very clear, but it could be an Auger process.¹⁹

C. Effect of Temperature on Total Lifetime of EHD

We have directly measured the EHD total lifetime between 1.95 and 4.35 °K. The results of these experiments are given in Fig. 9. At the same time, we have observed that, in this temperature range, the initial signal does not change with T . It is therefore clear that n_c does not vary appreciably

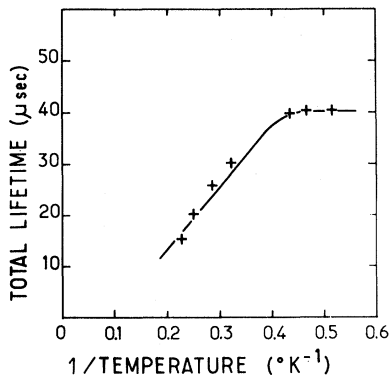


FIG. 9. Total lifetime of EHD vs $1/T$ for temperatures ranging from 1.95 to 4.25 °K.

between 1.95 and 4.35 °K. Consequently, τ_R^{EHD} is constant in this temperature range so that it was also possible to obtain the variation of τ^{EHD} with T by a measurement of the integrated luminescence of EHD in the same excitation conditions. The results are shown in Fig. 10. If we take into account the accuracy of the direct experimental determination of τ^{EHD} , the data represented in Figs. 9 and 10 are in good agreement.

We can interpret the variation of τ^{EHD} with T by two recombination mechanisms. One of these mechanisms take place into the drop volume and corresponds to $\tau^{\text{EHD}} \sim 40 \mu\text{sec}$,¹⁹ and the other one is related to the evaporation of FE at the drop surface. Let us note that the total lifetime τ^{FE} of FE is much shorter than $40 \mu\text{sec}$ ($\tau^{\text{FE}} \sim 5 \mu\text{sec}$). The experimental data show that these two contributions are nearly equal around 3 °K. This seems reasonable on the basis of the following calculation. Since τ^{FE} is much shorter than τ^{EHD} , the equality of these two contributions for a drop of radius r corresponds to

$$\frac{4}{3} \pi r^3 (n_c / \tau^{\text{EHD}}) = A T^2 4 \pi r^2 e^{-\phi / kT},$$

where A is the well-known Richardson constant and the work function ϕ for the emission of carriers from EHD is equal to 2.7 meV as determined by Pokrovskii and Svistunova.²⁵ This equation is satisfied for $T=3 \text{ °K}$ and $n_c = 2 \times 10^{17} \text{ cm}^{-3}$ if $r \sim 2 \mu$, which is a typical EHD radius.⁵

V. EXPERIMENTAL SITUATION IN SILICON

In Si the experiments which could clearly demonstrate the existence of EHD (photovoltaic detection^{4,5} and light scattering⁶) have not yet been achieved. However the recombination-radiation data² are quite similar to those obtained in Ge. In particular, the emission spectrum at 2 °K can

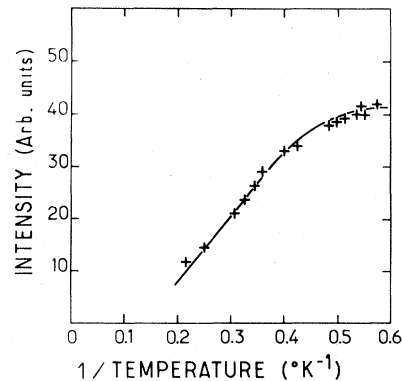


FIG. 10. Intensity of the integrated luminescence of EHD vs $1/T$ for temperatures ranging from 1.75 to 4.65 °K.

TABLE I. Values of the most important parameters relative to EHD in Ge and Si; R^* is obtained from Ref. 11 in Ge and from Ref. 27 in Si. The values of n_c are those which have been determined from experimental data. The inter-electron spacings r_s , $\langle E_{\text{kin}}^e \rangle + \langle E_{\text{kin}}^h \rangle$, and $\langle E_{\text{ex}}^e \rangle + \langle E_{\text{ex}}^h \rangle$ are calculated (Ref. 28) from the experimental values of n_c [for Ge, $m_e = 0.22 m_0$ (Ref. 29), $m_h = 0.31 m_0$ (Ref. 30), and $\epsilon = 15.4$ (Ref. 31); for Si, $m_e = 0.32 m_0$ (Ref. 32), $m_h = 0.54 m_0$ (Ref. 33), and $\epsilon = 11.4$ (Ref. 31)]. $\langle E_n \rangle_m - E_g$, which is negative, is also obtained from experimental results and its absolute value is given by the sum of the FE binding energy and of the distance between the EHD and the FE emission peaks (Refs. 2 and 14). $\langle E_{\text{cor}} \rangle$, which is equal to $\langle E_n \rangle_m - E_g - \langle E_{\text{kin}}^e \rangle - \langle E_{\text{kin}}^h \rangle - \langle E_{\text{ex}}^e \rangle - \langle E_{\text{ex}}^h \rangle$, is therefore determined here from experimental data. The last column of the table gives the theoretical values n_c^{th} of the critical density calculated from the simple theory developed here.

	R^* (meV)	n_c (cm ⁻³)	r_s	$\langle E_{\text{kin}}^e \rangle + \langle E_{\text{kin}}^h \rangle$ (meV)	$\langle E_{\text{ex}}^e \rangle + \langle E_{\text{ex}}^h \rangle$ (meV)	$\langle E_n \rangle_m - E_g$ (meV)	$\langle E_{\text{cor}} \rangle$ (meV)	n_c^{th} (cm ⁻³)
Ge	3.6	1.95×10^{17}	~ 3	3.7	-5.15	-8.2	-6.75	$\sim 6.8 \times 10^{16}$
Si	14.7	3.7×10^{18}	~ 3	14.7	-20.1	-29.7	-24.3	$\sim 1.2 \times 10^{18}$

be explained quite well⁷ with $n_c = 3.7 \times 10^{18} \text{ cm}^{-3}$.

If we call x the new entity responsible for that spectrum, the ratio of τ_R^{FE} and τ_R^x appear to be large as it is the case in Ge. This ratio is equal to about $25^{18, 26}$ in Si, and it is noteworthy that this fact can be easily explained only in the EHD model. From a theoretical point of view, the multivalley structure of the conduction band in Si (six valleys) is certainly favorable to the formation of EHD. All these considerations seem to show that EHD exist also in Si at low temperature. In this case, the short total lifetime²⁶ ($\sim 80 \text{ nsec}$) seems to be in agreement with an Auger process. Besides, one can easily compare the ratio of the Auger lifetimes in Ge and Si (which are of the order of 10^3) to the ratio of the corresponding n_c^2 (which is near 350) if we give to n_c its experimental value in both cases. Let us note that the agreement between these two ratios is rather satisfying.

VI. CONCLUSION

The existence of EHD is now well established in Ge and is likely in Si. In Table I are summarized the most important parameters for these two materials. The purpose of this table is also to show the order of magnitude of the mean correlation energy which is required to fit the experimental energy of EHD in Ge and in Si, though the existence of these drops is not actually proved in Si. Table I shows that $\langle E_{\text{cor}} \rangle$, which must be negative, is greater than $\langle E_{\text{kin}}^e \rangle + \langle E_{\text{kin}}^h \rangle$ by a factor smaller than 2 in both cases.

ACKNOWLEDGMENTS

The authors wish to thank Professor P. Nozières and Mrs. M. Combescot for helpful discussions and for communication of their results prior to publication. They are also very grateful to Professor P. Aigrain for his constant interest in that work.

[†]Part of this paper has been given at the Europhysics Conference on Metal-Insulator Transition and the Development of Narrow Energy Bands, Aussois, France, September 6-11, 1971 (unpublished).

*Laboratoire associé au C.N.R.S.

¹M. A. Lampert, Phys. Rev. Letters **1**, 450 (1958).

²J. R. Haynes, Phys. Rev. Letters **17**, 860 (1966).

³L. V. Keldysh, in *Proceedings of the Ninth International Conference on the Physics of Semiconductors*, Moscow, 1968, edited by S. M. Ryvkin and Yu. V. Shmartsev (Nauka, Leningrad, 1968), p. 1303.

⁴V. M. Asnin, A. A. Rogachev, and N. I. Sablina, Zh. Eksperim. i Teor. Fiz. Pis'ma v Redaktsiyu **11**, 162 (1970) [Sov. Phys. JETP Letters **11**, 99 (1970)].

⁵C. Benoît à la Guillaume, M. Voos, F. Salvan, J. M. Laurant, and A. Bonnot, Compt. Rend. **272B**, 236 (1971).

⁶Y. E. Pokrovskii and K. I. Svistunova, Zh. Eksperim. i Teor. Fiz. Pis'ma v Redaktsiyu **13**, 297 (1971) [Sov. Phys. JETP Letters **13**, 212 (1971)].

⁷Y. Pokrovsky, A. Kaminsky, and K. Svistunova, in *Proceedings of the Tenth International Conference on the Physics of Semiconductors*, Cambridge, Massachusetts,

1970, edited by S. P. Keller, J. C. Hensel, and F. Stern (U.S. AEC Division of Technical Information, Springfield, Va., 1970), p. 504.

⁸V. S. Vavilov, V. A. Zayats, and V. N. Murzin, Zh. Eksperim. i Teor. Fiz. Pis'ma v Redaktsiyu **10**, 304 (1969) [Sov. Phys. JETP Letters **10**, 192 (1969)].

⁹V. M. Asnin and A. A. Rogachev, Zh. Eksperim. i Teor. Fiz. Pis'ma v Redaktsiyu **14**, 494 (1971) [Sov. Phys. JETP Letters **14**, 338 (1971)].

¹⁰P. Nozières and M. Combescot (private communication).

¹¹E. F. Gross, V. I. Safarov, A. N. Titkov, and I. S. Shlimak, Zh. Eksperim. i Teor. Fiz. Pis'ma v Redaktsiyu **13**, 332 (1971) [Sov. Phys. JETP Letters **13**, 235 (1971)].

¹²M. Lax and J. J. Hopfield, Phys. Rev. **124**, 115 (1961).

¹³See, for example, A. W. Overhauser, Phys. Rev. **B 3**, 1888 (1971).

¹⁴Y. E. Pokrovskii and K. I. Svistunova, Zh. Eksperim. i Teor. Fiz. Pis'ma v Redaktsiyu **9**, 435 (1969) [Sov. Phys. JETP Letters **9**, 261 (1969)].

¹⁵C. Benoît à la Guillaume, F. Salvan, and M. Voos, *J. Luminescence* **1/2**, 315 (1970).

¹⁶It is noteworthy that one of the qualitative arguments used to distinguish between excitonic molecules and EHD is the kinetics of the new emission lines. In fact they are discrepancies between the results reported in Refs. 7 and 15, but in such experiments, one has to be very careful to the homogeneity of the excitation. In fact the problem of the kinetics in the EHD model is not yet fully resolved in our opinion.

¹⁷C. Benoît à la Guillaume and O. Parodi, in *Proceedings of the Fifth International Conference on Semiconductor Physics, Prague, 1960* (Academic, New York, 1961), p. 426.

¹⁸C. Benoît à la Guillaume, F. Salvan, and M. Voos, in Ref. 7, p. 516.

¹⁹C. Benoît à la Guillaume, M. Voos, and F. Salvan, *Phys. Rev. Letters* **27**, 1214 (1971).

²⁰We thank Dr. D. Adler for drawing our attention on that point.

²¹G. D. Pikus and G. L. Bir, *Fiz. Tverd. Tela* **1**, 1642 (1959) [*Sov. Phys. Solid State* **1**, 1502 (1960)].

²²I. Balslev, *Phys. Rev.* **143**, 636 (1966).

²³V. S. Bagaev, T. I. Galkina, and O. V. Gogolin,

in Ref. 7, p. 500.

²⁴J. C. Hensel and G. Feher, *Phys. Rev.* **129**, 1041 (1963).

²⁵Y. E. Pokrovskii and I. I. Svistunova, *Fiz. Tekhn. Poluprov.* **4**, 491 (1970) [*Sov. Phys. Semicond.* **4**, 409 (1970)].

²⁶J. D. Cuthbert, *Phys. Rev. B* **1**, 1552 (1970).

²⁷K. L. Shaklee and R. E. Nahory, *Phys. Rev. Letters* **24**, 942 (1970).

²⁸In the case of Si we have also used unpublished results of P. Nozières and M. Combescot to obtain the exact value of the mean exchange energies. They have shown that $\langle E_{ex}^e \rangle$ is reduced by a factor 0.94 and $\langle E_{ex}^h \rangle$ by a factor 0.88 when the anisotropy of the conduction band and the degeneracy of the valence band are taken into account.

²⁹B. W. Levinger and D. R. Frankl, *J. Phys. Chem. Solids* **20**, 281 (1961).

³⁰J. C. Hensel and K. Suzuki, in Ref. 7, p. 541.

³¹R. A. Faulkner, *Phys. Rev.* **184**, 713 (1969).

³²J. C. Hensel, H. Hasegawa and M. Nakayama, *Phys. Rev.* **138**, A225 (1965).

³³N. O. Lipari and A. Baldereschi [*Phys. Rev. B* **3**, 2497 (1971)] referred to unpublished results of P. Lawaetz.

Absorption and Electroabsorption of Trigonal Selenium near the Fundamental Absorption Edge

R. Fischer*

Physikalisches Institut der Universität Frankfurt/Main, Germany

(Received 27 May 1971)

The absorption spectrum and the spectrum of electroabsorption of vapor-grown trigonal Se platelets have been measured at various temperatures down to 2°K. The absorption curves for both $\vec{E} \parallel c$ and $\vec{E} \perp c$ show several steps at the onset of the absorption edge. No Urbach tail has been found. The steps are interpreted as arising from the indirect excitation of an exciton at 1.853 eV (low-temperature value) with several phonons. The electroabsorption spectra confirm the step structure within the absorption edge. Finally, it is shown that the luminescence of Se can also be explained with the same model.

I. INTRODUCTION

The band gap of trigonal selenium lies in the red part of the visible spectrum, at about 2 eV. This follows from optical properties of selenium single crystals.^{1,2} In spite of this advantage of an easy spectroscopy, great difficulties existed in measuring directly, i.e., by absorption measurements, whether the optical gap is direct or indirect. These difficulties arose mainly from the preparation of suitable single crystals: During these investigations both the absorption coefficient and the luminescence were found to be highly sensitive to pressure and deformation. Therefore no polishing may be applied to cleaved melt-grown crystals. On the other hand, vapor-grown crystals, which can be taken as-grown, were too thin to show fine structure

in the absorption edge at low absorption coefficients.³

Former band-structure calculations⁴ show the minimum band gap of selenium to be direct, but they do not exclude the alternative possibility, since the calculated bands are very flat in k space. Thus, small corrections would yield just the opposite result.

The most recent calculations⁵ give an indirect minimum band gap, though, of course, because of the flat bands, with the same restrictions.

Many spectroscopic methods have been applied to selenium in order to answer the question about the nature of the optical band gap. Absorption^{3,6} and reflection⁷⁻¹⁰ spectra and electroabsorption¹¹ and electroreflection¹² spectra have been experimentally studied. The absorption spectrum at He temperatures⁸ has been taken only from melt-grown